Journal of Zhejiang University-SCIENCE B (Biomedicine & Biotechnology)
ISSN 1673-1581 (Print); ISSN 1862-1783 (Online)
www.jzus.zju.edu.cn; www.springerlink.com
E-mail: jzus@zju.edu.cn

# Spontaneous activity in medial orbitofrontal cortex correlates with trait anxiety in healthy male adults*

Shao-wei XUE[†‡1,2,3], Tien-wen LEE[1,2,3,4], Yong-hu GUO[1,2,3]

[1]*Institutes of Psychological Sciences, Hangzhou Normal University, Hangzhou 311121, China*

[2]*Center for Cognition and Brain Disorders, Hangzhou Normal University, Hangzhou 311121, China*

[3]*Zhejiang Key Laboratory for Research in Assessment of Cognitive Impairments, Hangzhou 311121, China*

[4]*Department of Psychiatry, Dajia Lee's General Hospital, Lee's Medical Corporation, Taichung 43748, China*

[†]E-mail: xuedrm@126.com

Received Sept. 21, 2017; Revision accepted Dec. 4, 2017; Crosschecked July 6, 2018

**Abstract:** Medial orbitofrontal cortex (mOFC) abnormalities have been observed in various anxiety disorders. However, the relationship between mOFC activity and anxiety among the healthy population has not been fully examined. Here, we conducted a resting state functional magnetic resonance imaging (R-fMRI) study with 56 healthy male adults from the Nathan Kline Institute/Rockland Sample (NKI-RS) to examine the relationship between the fractional amplitude of low-frequency fluctuation (fALFF) signals and trait anxiety across the whole brain. A Louvain method for module detection based on graph theory was further employed in the automated functional subdivision to explore subregional correlates of trait anxiety. The results showed that trait anxiety was related to fALFF in the mOFC. Additionally, the resting-state functional connectivity (RSFC) between the right subregions of the mOFC and the precuneus was correlated with trait anxiety. These findings provided evidence about the involvement of the mOFC in anxiety processing among the healthy population.

**Key words:** Trait anxiety; Fractional amplitude of low-frequency fluctuation (fALFF); Medial orbitofrontal cortex; Precuneus; Functional connectivity

https://doi.org/10.1631/jzus.B1700481 **CLC number:** B845

## 1 Introduction

Anxiety is a psychological and physiological condition characterized by an unpleasant feeling of inner turmoil—and if left unregulated or inappropriately regulated, it reduces the quality of everyday life and may facilitate the development of affective disorders (Scheinost et al., 2013; Kim et al., 2016). This anxiety condition is characterized by a combination of physiological, behavioral, and cognitive components and manifests itself in two recognizable ways—state or trait (Spampinato et al., 2009). State anxiety can be defined as a temporary disturbing emotional arousal as a result of the recognition of a disturbing stimulus, while trait anxiety corresponds to worrying about future events and reflects a stable tendency to respond consistently with state anxiety when faced with threatening demands or dangers (Spielberger et al., 1983). Because trait anxiety is generally considered a stable personality trait and varies among individuals, it is an ideal tool for exploring the brain–anxiety relationship (Raymond et al., 2017).

Many previous studies have demonstrated that the neural correlates of anxiety implicate the

‡ Corresponding author

* Project supported by the Natural Science Foundation of Zhejiang Province (No. LY17H180007), the Scientific Research Fund of Zhejiang Education Department (No. Y201431735), and the Hangzhou Science and Technology Commission Foundation (No. 20170533B06), China

ORCID: Shao-wei XUE, https://orcid.org/0000-0001-5441-4522

orbitofrontal cortex (OFC). An early study using in vivo proton magnetic resonance spectroscopy (MRS) reported that the total concentration of two OFC chemicals (*N*-acetylaspartate and glutamine) in healthy humans was strongly correlated with the anxiety total score (Grachev and Apkarian, 2000). Evidence from structural magnetic resonance imaging (MRI) studies has indicated that reduced volumes in the medial OFC (mOFC) were associated with anxiety disorders. For example, a previous study found reductions of OFC volumes in survivors of cancer with posttraumatic stress disorder (PTSD) when they were compared to cancer survivors without PTSD and to a healthy group (Hakamata et al., 2007). Another study observed volume reductions of the right posterior-mOFC among panic disorder individuals compared to healthy controls (Scheinost et al., 2013). Previous functional imaging studies have demonstrated that abnormal mOFC activation was detected across some clinical anxiety disorders (Shin and Liberzon, 2010). Another functional MRI (fMRI) study revealed increased activity during high-anxiety imagery compared to neutral-anxiety imagery in the patients with panic disorder in the OFC when compared to control individuals (Bystritsky et al., 2001). Recently, a resting-state functional near-infrared spectroscopy (fNIRS) study demonstrated that associations in the functional connectivity between the left inferior frontal gyrus and the OFC were related to anxiety in chronic heroin users (Ieong and Yuan, 2017). Although there are many studies about the involvement of the (medial) OFC in pathological anxiety, the number of studies that have investigated the mOFC correlates of anxiety remains sparse, particularly studies considering healthy populations.

The mOFC, which occupies the cortex on the orbital surface of the frontal lobe, is ideally positioned to extensively connect to other brain areas. This area projects to the ventral striatum, indicating that it plays a role in the circuitry of reward-oriented behavior (Heekeren et al., 2007). It projects to the amygdala, the hypothalamus, and the hippocampus, and these projections are thought to play a notable role in the emotional decision-making process (Milad and Rauch, 2007). Previous studies have found that anxiety-related behaviors may involve top-down regulatory influences from the OFC to the amygdala (Banks et al., 2007; Kim et al., 2011), or the OFC may play a crucial role in the modulation of anxiety via the amygdala (Milad et al., 2006; Liao et al., 2010). Besides, the OFC has also been found to have the reduction effect on resting-state functional connectivity (RSFC) with the amygdala in social anxiety disorder (Hahn et al., 2011).

Recently, advances in resting state fMRI (R-fMRI) methodology have facilitated the identification of brain states in various conditions (such as eyes-opened and eyes-closed conditions) and abnormal intrinsic brain activity in various neurological and neuropsychiatric diseases (Zhang and Raichle, 2010). The amplitude of low-frequency fluctuation (ALFF) measures the magnitude of the spontaneous brain blood oxygenation level-dependent (BOLD) signal and has been suggested to be associated with local neuronal activity (Zang et al., 2007). As a normalized index of ALFF, fractional ALFF (fALFF) can attenuate the biases of physiological noise and provide more accurate measures (Zou et al., 2008). Previous studies found alterations in fALFF in various brain disorders such as anxiety disorder (Hahn et al., 2011; Lai and Wu, 2015) and schizophrenia (Hoptman et al., 2010).

The present research investigated how the OFC represents brain–anxiety associations in healthy adults. For the first time, we identified areas that showed significant correlations between trait anxiety scores of the State-Trait Anxiety Inventory (STAI) (Spielberger et al., 1983) and the fALFF of R-fMRI signals (Zou et al., 2008). A seed-based RSFC analysis was then performed, in which the placement of seed regions of interest (ROIs) was determined on the automated functional subdivision within a mOFC mask and their RSFC associations with trait anxiety scores were characterized. We hypothesized that there would exist a significant correlation between trait anxiety and spontaneous activity in the mOFC and different correlations between trait anxiety scores and various mOFC subregional RSFCs.

## 2 Materials and methods

### 2.1 Participants

A group of 56 healthy, right-handed male adults (mean age, 42.75 years; standard deviation, 18.87 years; age range, 19–82 years) were selected from the Nathan

Kline Institute/Rockland Sample (NKI-RS) and were publicly available at the International Neuroimaging Data-Sharing Initiative (INDI) online database (http://fcon_1000.projects.nitrc.org/indi/pro/nki.html). The initial release of the NKI-RS included 207 participants who finished brain MRI scans, diagnostic psychiatric interviews, and psychiatric assessments. A total of 126 subjects were not diagnosed with a mental illness. Twenty-five participants under 18 years of age were not selected. These data were collected according to protocols approved by the Institutional Review Board of the Nathan Kline Institute (New York, USA) and written informed consent was obtained from each participant (Nooner et al., 2012).

### 2.2 Anxiety assessment

Anxiety levels were assessed with the STAI for adults, which is an introspective psychological inventory consisting of 40 self-report items pertaining to anxiety affect (Spielberger et al., 1983). The STAI is divided into two sections, each with 20 questions. The first subscale measures state anxiety, and the second measures trait anxiety. Both use ratings on a 4-point scale: 1, almost never; 2, sometimes; 3, often; 4, almost always. Scores range from 20 (low trait anxiety) to 80 (high trait anxiety), with higher scores suggesting greater symptomatology of anxiety. Trait anxiety is defined as a stable aspect of personality that describes an individual's tendency to respond to a situation with anxiety, while state anxiety refers to a transitory state of emotional arousal. The STAI can be used in clinical settings to diagnose anxiety and to distinguish it from depressive syndromes. In the current study, one subject was excluded before further analyses, due to missing STAI values. The mean score on the STAI trait anxiety scale was 30.96 (standard deviation: 10.00), and higher scores on the STAI indicated higher trait anxiety levels. The STAI is a self-report measure and takes approximately 10 min.

### 2.3 Image acquisition and preprocessing

All MRI images, which covered the whole brain, were acquired by a 3.0 Tesla Siemens MAGNETOM TrioTim scanner (Siemens AG, Medical Solutions, Erlangen, Germany). The R-fMRI scans were then collected using an echo-planar imaging (EPI) sequence (repetition time (TR)=2500 ms, echo time (TE)=30 ms, flip angle (FA)=80°, field of view (FOV)=216 mm×216 mm, voxel size=3.0 mm×3.0 mm×3.0 mm, number of slices=38). A total of 260 whole-brain EPI images were collected for approximately 650 s. A high-resolution T1-weighted anatomical image in the sagittal orientation was acquired using a magnetization-prepared rapid gradient echo (MP-RAGE) sequence (TR=2500 ms, TE=3.5 ms, FA=8°, FOV=256 mm×256 mm, voxel size=1.0 mm×1.0 mm×1.0 mm, number of slices=192) and was used to facilitate the anatomical description and to register R-fMRI data. The participants were instructed to relax with their eyes closed but not fall asleep and remain as motionless as possible during the scanning. The detailed scanning protocol can be found at the following webpage: http://fcon_1000.projects.nitrc.org/indi/pro/nki.html.

Functional image preprocessing was performed using the Data Processing Assistant for Resting-State fMRI (DPARSF; http://www.restfmri.net) and Statistical Parametric Mapping (SPM8, Wellcome Department, London, UK; http://www.fil.ion.ucl.ac.uk/spm). For each dataset, the first ten functional volumes were discarded to allow for magnetization equilibration effects and the adaptation of the participants to the circumstances. The remaining images for the further process were first corrected for time delay between slices and were then realigned to the first volume for head-motion correction. The realigning step provided a record of head motions by estimating the translations in each direction and the rotations in angular motion about each axis for each of the consecutive volumes. The images were normalized into a standard stereotactic space as defined by the Montreal Neurological Institute (resampling voxel size=3 mm×3 mm×3 mm) and smoothed with a 4-mm full-width at half-maximum Gaussian kernel. Finally, all fMRI time series underwent temporal bandpass filtering (between 0.01 and 0.1 Hz) and nuisance signal removal from the ventricles and deep white matter, and any effects of head motion were regressed out. Global signals were not regressed out. For functional images, all participants included in the study showed a mean frame-wise displacement of less than 0.5 mm (Power et al., 2012).

### 2.4 fALFF analysis

The fALFF was computed using DPARSF software (Yan and Zang, 2010). Briefly, the time

series of each voxel was transformed to obtain the power spectrum using a fast Fourier transform (FFT). The square root of the power spectrum was calculated at each frequency and averaged across 0.01–0.1 Hz for each voxel (Biswal et al., 1995; Fox and Raichle, 2007). fALFF was calculated using the ratio of the power spectrum of low-frequency (0.01 to 0.1 Hz) to that of the entire frequency range (Zuo et al., 2010). The value of each voxel was standardized by dividing the full-brain mean fALFF values to reduce the global effects of variability across participants (Zou et al., 2008). The global mean fALFF was calculated only within the brain, with the background and other tissues outside the brain removed.

### 2.5 Automated functional subdivision in the mOFC

To automatically partition the mOFC into subregions, we applied a Louvain method for module detection based on graph theory (Xia et al., 2014). BOLD signal time courses of all voxels were extracted within a bilateral mOFC mask defined by the automated anatomical labelling (AAL) atlas (Tzourio-Mazoyer et al., 2002), which was included in the MRIcro software package (http://www.sph.sc.edu/comd/rorden/mricro.html). Their pairwise Pearson's correlation coefficients were computed to develop a correlation matrix. The backbone of the mean matrix across all participants was then constructed by applying a nonparametric method of locally adaptive network sparsification (Foti et al., 2011). The module detection algorithm (Newman, 2006) was applied to the backbone to parcellate the mOFC into composite modules for a functional connectivity analysis. RSFC for each participant was calculated as the Pearson correlation coefficient between the mean resting-state BOLD time series of each seed ROI and other voxels in the whole brain (Biswal et al., 1997).

### 2.6 Statistical analysis

To locate anxiety-related areas, we conducted Pearson's correlation analysis between fALFF measures and the STAI anxiety scores in whole brain on a voxel by voxel basis. Multiple comparison correction was performed using Gaussian Random Field (GRF) theory by $Z>2.6$, voxel $P<0.005$, and a GRF cluster-corrected threshold of $P<0.05$ with a cluster size of 10 voxels (Worsley, 2001). Subsequently, the mean fALFF of each mOFC subregion was extracted by averaging the fALFF of all the voxels belonging to that subregion. The subregional mean fALFF was used to compute correlation coefficients with the anxiety scores. The RSFC of each mOFC subregion was generated by calculating Pearson's correlation between the mean BOLD time series of each subregion and each voxel in the whole brain. To assess the mOFC subregion-anxiety relationship, we further performed voxel-based Pearson's correlation analysis between the RSFC of each mOFC subregion and anxiety scores. The significance threshold was set to voxel $P<0.005$, and a GRF cluster-corrected threshold of $P<0.05$ with a cluster size of 10 voxels.

## 3 Results

### 3.1 Correlations between STAI anxiety scores and voxel-wise fALFF

As shown in Fig. 1, we found that significant ($P<0.05$, corrected) positive correlations between fALFF values and STAI trait anxiety scores were primarily located in the right medial part of the orbitofrontal cortex (peak MNI (Montreal Neurological Institute) coordinates: $x=6$, $y=57$, $z=-12$, correlation coefficient ($r$)=0.6, cluster size=33 voxels), which extended to the right anterior cingulate gyrus and the medial part of the superior frontal gyrus. Besides, several brain regions showing negative correlations included the right superior temporal pole, right hippocampus, and calcarine sulcus ($P<0.05$, corrected).

### 3.2 Functional parcellation within the mOFC

To examine the subregional specificity of the relationship between fALFF and STAI trait anxiety, the module detection method was used based on the BOLD time courses of all voxels within the whole mOFC. The modularity structure was observed (modularity value ($Q$)=0.6), and seven subregions were detected in both hemispheres (Fig. 2a; ROI 1, black; ROI 2, magenta; ROI 3, red; ROI 4, yellow; ROI 5, cyan; ROI 6, green; ROI 7, blue). The mean time series of each mOFC subregion was extracted for further pairwise correlation analysis. Based on a mean correlation matrix (7×7; Fig. 2b) across all participants, an additional hierarchical clustering analysis (Xia et al., 2014; Wang et al., 2015) was used to classify the seven mOFC subregions into two zones along

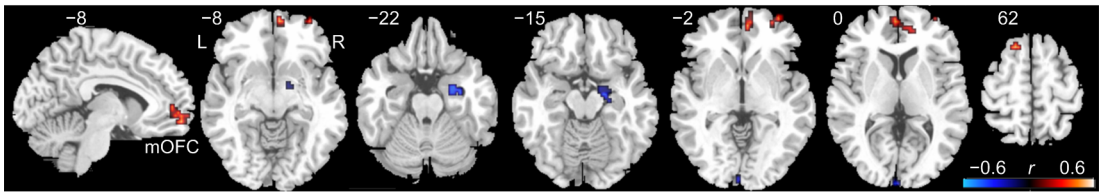


**Fig. 1 Cluster showing significant correlations between the fractional amplitude of low-frequency fluctuation (fALFF) and State-Trait Anxiety Inventory (STAI) trait anxiety scores in healthy adults**

The colors represent correlation coefficients ($r$) ($P$<0.05, corrected). mOFC: medial orbitofrontal cortex; L: left side; R: right side (Note: for interpretation of the references to color in this figure legend, the reader is referred to the web version of this article)

an anterior-to-posterior/ventral gradient (Fig. 2c; the anterior zone: ROIs 1, 2, 3; the posterior zone: ROIs 4, 5, 6, 7). As presented in Fig. 2d, the mean subregional fALFF values were positively correlated with STAI trait anxiety values (ROI 1, $r$=0.14, $P$=0.3; ROI 2, $r$=0.2, $P$=0.13; ROI 3, $r$=0.25, $P$=0.07; ROI 4, $r$=0.25, $P$=0.07; ROI 5, $r$=0.31, $P$=0.019; ROI 6, $r$=0.23, $P$=0.087; ROI 7, $r$=0.24, $P$=0.07).

### 3.3 Voxel-wise correlation maps between the RSFC of each mOFC subregion and STAI trait anxiety scores

Voxel-wise correlation maps between the RSFC of seven mOFC subregions and STAI trait anxiety scores are illustrated in Fig. 3 and Table 1. In addition to adjacent prefrontal regions of the mOFC (such as the inferior and superior frontal gyrus), we found that significant ($P$<0.05, corrected) positive correlations between trait anxiety scores and subregional RSFC values of ROIs 2, 5, 6 and 3 were mainly involved in the precuneus. ROIs 2, 4, 5, 6 and 7 showed negative correlations in the inferior frontal gyrus and positive correlations in the left insula. ROIs 1, 3, 5, 6 and 7 showed positive correlations in the superior frontal gyrus.

## 4 Discussion

In the current study, the correlation between spontaneous activity of the mOFC and trait anxiety was found in the healthy male population. The module detection method was further employed in automated functional subdivisions to explore the subregional correlates of anxiety. We found that the RSFC between the right mOFC and the precuneus was correlated with trait anxiety. These findings extend the findings of previous studies on the association between the mOFC and anxiety in two ways.

First, we found that spontaneous activity of the mOFC measured with the fALFF was correlated with trait anxiety scores. Trait anxiety represents an individual's generalized and long-lasting predisposition marked by a tendency to view a situation as more dangerous than it is. People who suffer high trait anxiety might react to the stimulus or condition with excessive fear, despite the unrealistic likelihood of a catastrophic outcome (Spielberger et al., 1983). Elevated levels of trait anxiety are a risk factor for the development of clinical anxiety disorders (Chambers et al., 2004). Furthermore, this personality trait of anxiety may be linked to brain mechanisms that underlie stress and anxiety processing (Gawda and Szepietowska, 2016). Previous studies have indicated that the OFC is involved in the regulation of the neural architecture that mediates the basic response to threat, i.e. the amygdala and the hypothalamus (Blair et al., 2005). Lesions of the OFC presumably disrupt the downregulation of this neural architecture such that the individual is more likely to express the extreme reaction to a threat (reactive aggression) rather than a more appropriate action, such as freezing (Blair, 2007). In the current study, our research interests focused on how interindividual differences in trait anxiety were related to interindividual variability of local activity of the mOFC in healthy male adults and the RSFC of its different subdivisions. These results indicated that healthy male adults with higher anxiety scores showed stronger mOFC activity. One possibility is that these subjects with high anxiety require high intensity brain activities to deal with anxiety and further avoid it becoming pathological anxiety and individuals with low anxiety showed little mOFC activity because it was not being recruited (Spampinato et al., 2009; Qiu et al., 2015; Tian et al., 2016; Wang et al., 2017). Unregulated or inappropriate anxiety control and inhibition due to deficient mOFC function might lead to psychopathology (Shiba et al., 2016).

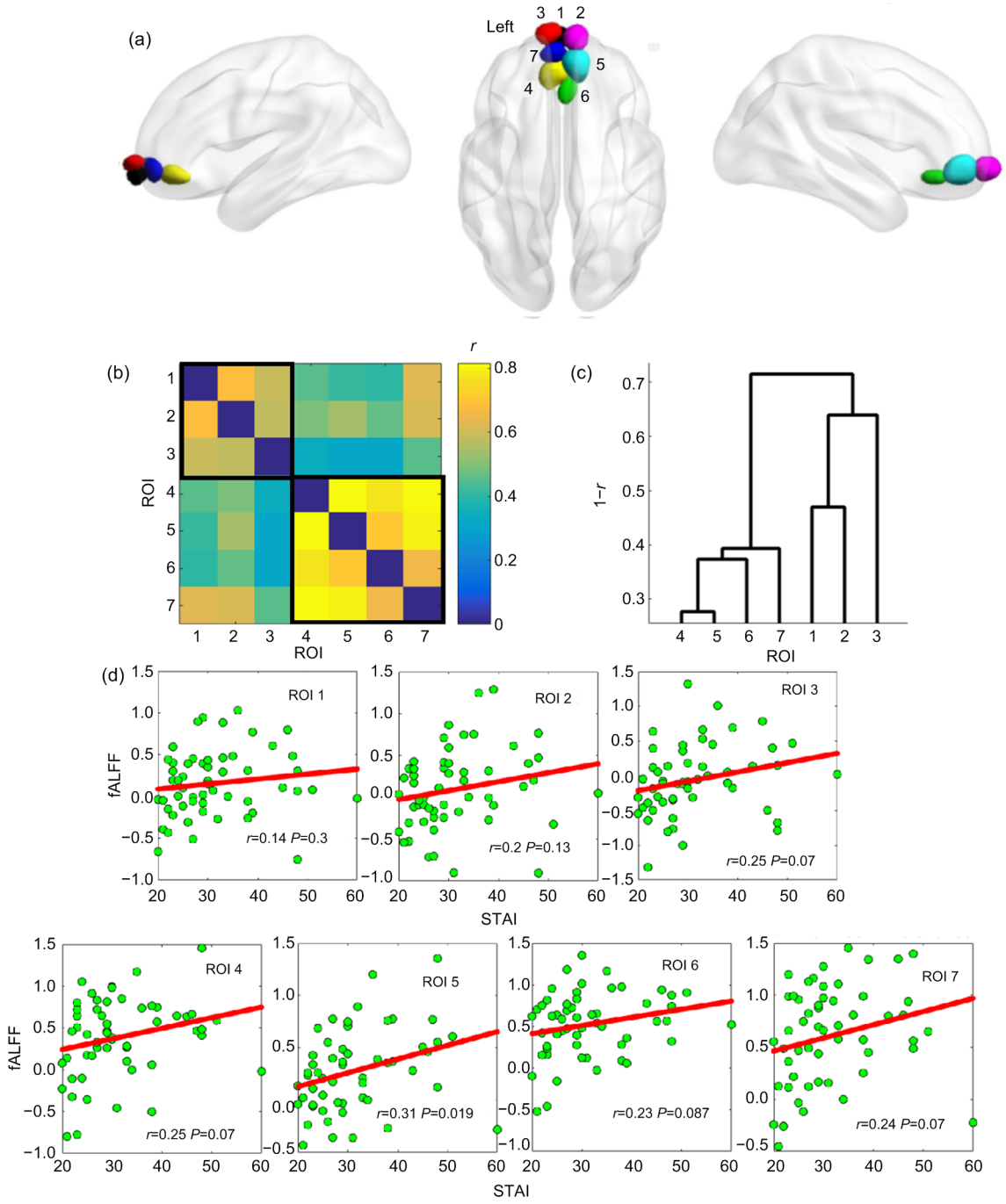


**Fig. 2 mOFC subregions and their relationships between fALFF and trait anxiety scores**

(a) Automated detection of seven mOFC subregions. (b) Mean pairwise correlation (*r*) matrix of subregional BOLD time courses. (c) Hierarchical clustering based on the correlation matrix-revealed two zones. (d) Scatterplots for the relationship between fALFF and STAI values in seven mOFC subregions. ROI, region of interest; fALFF, fractional amplitude of low-frequency fluctuation; STAI, State-Trait Anxiety Inventory

Second, the mOFC was further automatically divided into anterior and posterior zones based on its BOLD time courses rather than its anatomical profile. However, the differential relationships between the RSFC of the mOFC subregions and trait anxiety suggest that different mOFC subregions may relate to distinct functions; in particular, there is likely heterogeneity in the mOFC functional integration of anxiety processing across left and right anatomical subdivisions rather than functional ones. Previous evidence

**Table 1 Correlations between RSFC of seven mOFC subregions and STAI trait anxiety scores in healthy man adults**

| Seed region | Anatomical region | Cluster size (voxel) | Peak *r*-value | Peak MNI coordinate (mm) | | |
|---|---|---|---|---|---|---|
| | | | | *x* | *y* | *z* |
| ROI 1 | R: superior frontal gyrus (medial) | 17 | 0.51 | 15 | 57 | 0 |
| | L: superior frontal gyrus (medial) | 10 | 0.47 | −9 | 69 | 6 |
| ROI 2 | L: precuneus | 65 | 0.52 | 0 | −75 | 39 |
| | R: rectus | 26 | 0.56 | 6 | 63 | −15 |
| | R: olfactory | 10 | 0.46 | 15 | 9 | −15 |
| | L: inferior frontal gyrus (orbital) | 19 | −0.50 | −33 | 36 | −12 |
| | R: putamen | 14 | −0.45 | 30 | 18 | 0 |
| | L: hippocampus | 14 | −0.51 | −18 | −39 | 6 |
| | L: insula | 32 | −0.44 | −27 | 15 | 12 |
| ROI 3 | L: precuneus | 14 | 0.48 | −15 | −60 | 30 |
| | L: superior frontal gyrus (medial) | 72 | 0.53 | −9 | 51 | 6 |
| | L: superior frontal gyrus (dorsal) | 10 | 0.43 | −30 | 39 | 39 |
| | R: precentral gyrus | 11 | −0.47 | 60 | 6 | 15 |
| ROI 4 | L: insula | 52 | −0.47 | −36 | 18 | 0 |
| | L: middle frontal gyrus (orbital) | 20 | −0.53 | 24 | 36 | −18 |
| | R: rolandic operculum | 16 | −0.44 | 63 | 6 | 6 |
| | L: inferior frontal gyrus (triangular) | 14 | −0.41 | −57 | 3 | 12 |
| | R: superior temporal gyrus | 16 | −0.43 | 69 | −33 | 18 |
| | R: postcentral gyrus | 15 | −0.45 | 66 | −12 | 30 |
| ROI 5 | L: precuneus | 52 | 0.55 | −3 | −78 | 51 |
| | R: precuneus | 29 | 0.51 | 3 | −57 | 63 |
| | L: superior frontal gyrus (dorsal) | 13 | 0.51 | −18 | 60 | 0 |
| | R: inferior frontal gyrus (orbital) | 15 | −0.44 | 39 | 33 | −15 |
| | L: inferior frontal gyrus (orbital) | 17 | −0.48 | −36 | 39 | −12 |
| | L: inferior frontal gyrus (triangular) | 11 | −0.45 | 57 | 24 | 27 |
| | L: insula | 21 | −0.44 | −33 | 18 | 0 |
| | R: postcentral gyrus | 20 | −0.47 | 66 | −9 | 30 |
| ROI 6 | L: precuneus | 27 | 0.47 | 0 | −78 | 45 |
| | L: superior frontal gyrus (dorsal) | 51 | 0.52 | −12 | 69 | 9 |
| | L: olfactory | 33 | 0.48 | −3 | −99 | −9 |
| | L: insula | 49 | −0.48 | −36 | 18 | 0 |
| | L: inferior frontal gyrus (orbital) | 10 | −0.48 | −33 | 36 | −12 |
| ROI 7 | L: superior frontal gyrus (medial) | 25 | 0.54 | −15 | 60 | 0 |
| | L: superior frontal gyrus (medial) | 17 | 0.48 | −9 | 54 | 6 |
| | R: inferior frontal gyrus (triangular) | 15 | −0.45 | 48 | 45 | −9 |
| | L: inferior frontal gyrus (triangular) | 11 | −0.50 | −39 | 33 | 9 |
| | L: inferior frontal gyrus (operculum) | 12 | −0.41 | −57 | 3 | 12 |
| | R: precentral gyrus | 12 | −0.44 | 63 | 6 | 18 |
| | L: insula | 43 | −0.47 | −36 | 15 | 0 |

RSFC, resting-state functional connectivity; L, left side; R, right side; *r*: correlation coefficient. MNI, Montreal Neurological Institute. Significance level was defined at voxel $P<0.005$, and a GRF cluster-corrected threshold of $P<0.05$ with a cluster size of 10 voxels

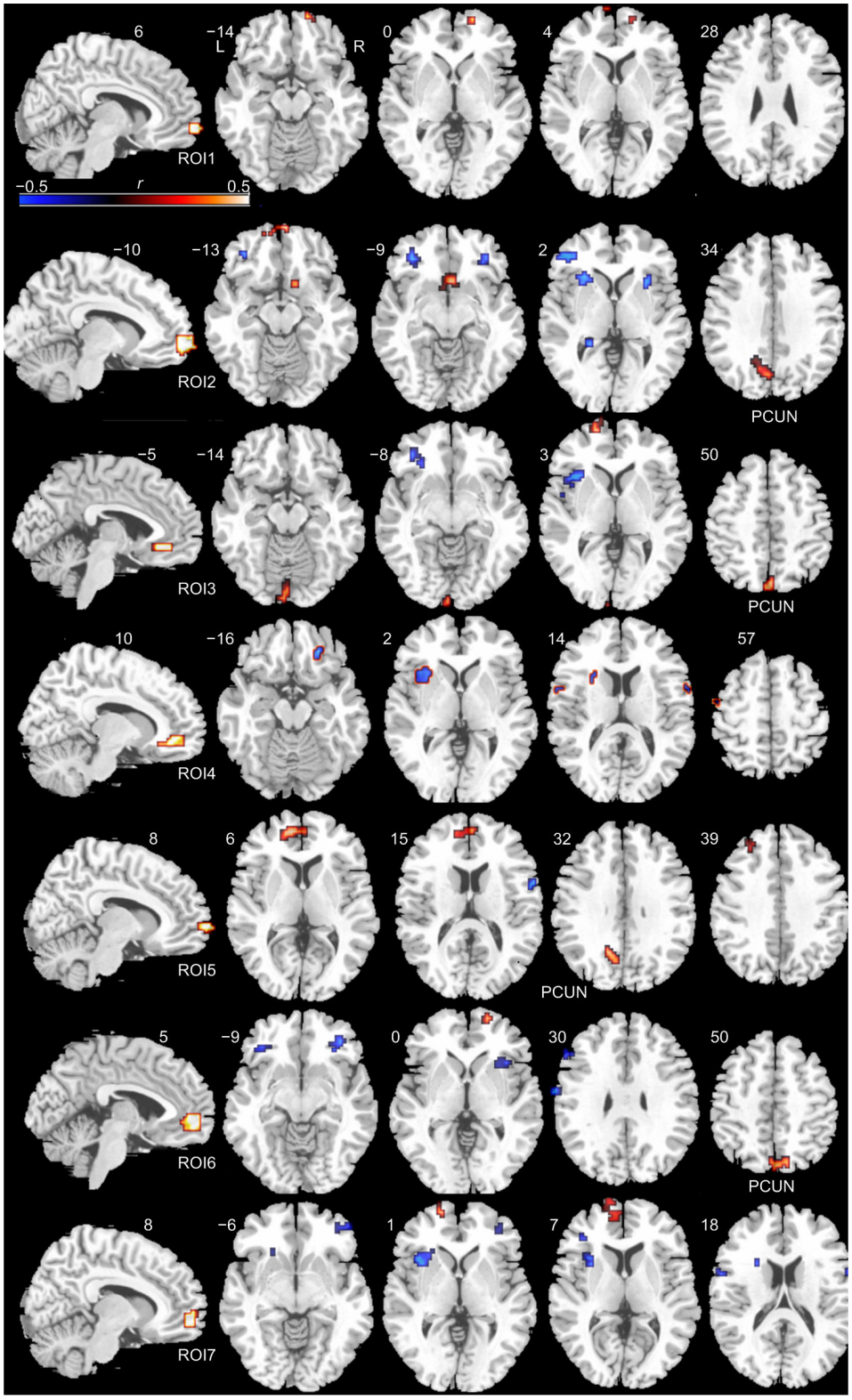


**Fig. 3 Voxel-wise correlation maps between the RSFC of each mOFC subregion and STAI trait anxiety scores**

The first column shows the mOFC subregions. The other columns show voxel-wise correlation maps of each mOFC subregion. Hot colours represent positive correlations, whereas cold colours represent negative correlations (voxel $P<0.005$, and a GRF cluster-corrected threshold of $P<0.05$ with a cluster size of 10 voxels). ROI: region of interest; PCUN: precuneus; L: left side; R: right side; colour bar represents *r*-values (Note: for interpretation of the references to color in this figure legend, the reader is referred to the web version of this article)

has shown that the OFC is a heterogeneous structure consisting of several subregions, with each subregion exhibiting distinct structural and functional connectivity patterns (Kahnt et al., 2012; Liu et al., 2015), but the contribution of the left/right subregions of the mOFC to anxiety processing and the nature of these functional distinctions remain unclear. Here, we found that coupling between the right mOFC and the precuneus was correlated with trait anxiety, whereas there were few voxels showing significant correlation in the RSFC between the left mOFC and the precuneus and trait anxiety. These results indicated that the left mOFC might differ from the right mOFC in anxiety processing.

The mOFC and precuneus are two central components of the default mode network (Raichle et al., 2001; Buckner et al., 2008) and have also been identified as critical hubs in human whole-brain structural and functional networks (Greicius et al., 2003). The precuneus plays an important role in processing emotional evaluation and regulation (Maddock et al., 2003). Furthermore, the precuneus and the adjacent posterior cingulate cortex (PCC) have been implicated in social and general anxiety (Hahn et al., 2011). For example, a previous study found increased activity in the precuneus in response to threat-related stimuli in patients with panic disorder (Zhao et al., 2007). Another study found that reduced connectivity between the amygdala and the precuneus/PCC was associated with higher state anxiety in adults with anxiety disorders (Hamm et al., 2014). We found associations between the connections between the anterior/posterior default mode network (DMN) and anxiety and provided evidence from different perspectives that the DMN might relate to anxiety.

Several limitations warrant further consideration. First, we have only examined a healthy male population. Recent studies have paid greater attention to individuals with anxiety disorder (Kent et al., 2005; Scheinost et al., 2013). Further investigation of the clinical population would provide new insights into the pathophysiology of anxiety disorder. Second, the module detection method successfully parcellated the whole mOFC into spatially coherent functionally homogeneous clusters based on R-fMRI data. Future work will compare this functionally derived parcellation against those derived from anatomy and diffusion tensor imaging. Third, another methodological consideration relates to mOFC definitions. The mOFC mask in this study was defined by the AAL atlas. Arguably, a more fine-grained mask of the medial part of the orbitofrontal cortex could be constructed based on cytoarchitectural features or other atlases.

In summary, our study showed that spontaneous activity of the mOFC was associated with trait anxiety in a healthy population, and the RSFC between the right mOFC and the precuneus related to trait anxiety. Our findings suggest that the mOFC is an anxiety-related region in healthy participants and could serve as a link to the neurobiology of anxiety disorders.

## Compliance with ethics guidelines

Shao-wei XUE, Tien-wen LEE, and Yong-hu GUO declare that they have no conflict of interest.

All procedures followed were in accordance with the ethical standards of the responsible committee on human experimentation (institutional and national) and with the Helsinki Declaration of 1975, as revised in 2008 (5). Informed consent was obtained from all patients for being included in the study.

## References

Banks SJ, Eddy KT, Angstadt M, et al., 2007. Amygdala-frontal connectivity during emotion regulation. *Soc Cogn Affect Neurosci*, 2(4):303-312. https://doi.org/10.1093/scan/nsm029

Biswal B, Yetkin FZ, Haughton VM, et al., 1995. Functional connectivity in the motor cortex of resting human brain using echo-planar MRI. *Magn Reson Med*, 34(4):537-541. https://doi.org/10.1002/mrm.1910340409

Biswal BB, van Kylen J, Hyde JS, 1997. Simultaneous assessment of flow and BOLD signals in resting-state functional connectivity maps. *NMR Biomed*, 10(4-5): 165-170. https://doi.org/10.1002/(SICI)1099-1492(199706/08)10:4/5<165::AID-NBM454>3.0.CO;2-7

Blair J, Mitchell D, Blair K, 2005. The Psychopath: Emotion and the Brain. Blackwell Publishing, Oxford, p.81-86.

Blair RJR, 2007. Dysfunctions of medial and lateral orbitofrontal cortex in psychopathy. *Ann NY Acad Sci*, 1121(1): 461-479. https://doi.org/10.1196/annals.1401.017

Buckner RL, Andrews-Hanna JR, Schacter DL, 2008. The brain's default network: anatomy, function, and relevance to disease. *Ann NY Acad Sci*, 1124(1):1-38. https://doi.org/10.1196/annals.1440.011

Bystritsky A, Pontillo D, Powers M, et al., 2001. Functional MRI changes during panic anticipation and imagery exposure. *Neuroreport*, 12(18):3953-3957. https://doi.org/10.1097/00001756-200112210-00020

Chambers JA, Power KG, Durham RC, 2004. The relationship between trait vulnerability and anxiety and depressive diagnoses at long-term follow-up of generalized anxiety disorder. *J Anxiety Disord*, 18(5):587-607. https://doi.org/10.1016/j.janxdis.2003.09.001

Foti NJ, Hughes JM, Rockmore DN, 2011. Nonparametric sparsification of complex multiscale networks. *PLoS ONE*, 6(2):e16431. https://doi.org/10.1371/journal.pone.0016431

Fox MD, Raichle ME, 2007. Spontaneous fluctuations in brain activity observed with functional magnetic resonance imaging. *Nat Rev Neurosci*, 8(9):700-711. https://doi.org/10.1038/nrn2201

Gawda B, Szepietowska E, 2016. Trait anxiety modulates brain activity during performance of verbal fluency tasks. *Front Behav Neurosci*, 10:10. https://doi.org/10.3389/fnbeh.2016.00010

Grachev ID, Apkarian AV, 2000. Anxiety in healthy humans is associated with orbital frontal chemistry. *Mol Psychiatry*, 5(5):482-488. https://doi.org/10.1038/sj.mp.4000778

Greicius MD, Krasnow B, Reiss AL, et al., 2003. Functional connectivity in the resting brain: a network analysis of the default mode hypothesis. *Proc Natl Acad Sci USA*, 100(1): 253-258. https://doi.org/10.1073/pnas.0135058100

Hahn A, Stein P, Windischberger C, et al., 2011. Reduced resting-state functional connectivity between amygdala and orbitofrontal cortex in social anxiety disorder. *Neuroimage*, 56(3):881-889. https://doi.org/10.1016/j.neuroimage.2011.02.064

Hakamata Y, Matsuoka Y, Inagaki M, et al., 2007. Structure of orbitofrontal cortex and its longitudinal course in cancer-related post-traumatic stress disorder. *Neurosci Res*, 59(4):383-389. https://doi.org/10.1016/j.neures.2007.08.012

Hamm LL, Jacobs RH, Johnson MW, et al., 2014. Aberrant amygdala functional connectivity at rest in pediatric anxiety disorders. *Biol Mood Anxiety Disord*, 4(1):15. https://doi.org/10.1186/s13587-014-0015-4

Heekeren HR, Wartenburger I, Marschner A, et al., 2007. Role of ventral striatum in reward-based decision making. *Neuroreport*, 18(10):951-955. https://doi.org/10.1097/WNR.0b013e3281532bd7

Hoptman MJ, Zuo XN, Butler PD, et al., 2010. Amplitude of low-frequency oscillations in schizophrenia: a resting state fMRI study. *Schizophr Res*, 117(1):13-20. https://doi.org/10.1016/j.schres.2009.09.030

Ieong HFH, Yuan Z, 2017. Abnormal resting-state functional connectivity in the orbitofrontal cortex of heroin users and its relationship with anxiety: a pilot fNIRS study. *Sci Rep*, 7:46522. https://doi.org/10.1038/srep46522

Kahnt T, Chang LJ, Park SQ, et al., 2012. Connectivity-based parcellation of the human orbitofrontal cortex. *J Neurosci*, 32(18):6240-6250. https://doi.org/10.1523/JNEUROSCI.0257-12.2012

Kent JM, Coplan JD, Mawlawi O, et al., 2005. Prediction of panic response to a respiratory stimulant by reduced orbitofrontal cerebral blood flow in panic disorder. *Am J Psychiatry*, 162(7):1379-1381. https://doi.org/10.1176/appi.ajp.162.7.1379

Kim MJ, Gee DG, Loucks RA, et al., 2011. Anxiety dissociates dorsal and ventral medial prefrontal cortex functional connectivity with the amygdala at rest. *Cereb Cortex*, 21(7):1667-1673. https://doi.org/10.1093/cercor/bhq237

Kim MJ, Brown AC, Mattek AM, et al., 2016. The inverse relationship between the microstructural variability of amygdala-prefrontal pathways and trait anxiety is moderated by sex. *Front Syst Neurosci*, 10:93. https://doi.org/10.3389/fnsys.2016.00093

Lai CH, Wu YT, 2015. The patterns of fractional amplitude of low-frequency fluctuations in depression patients: the dissociation between temporal regions and fronto-parietal regions. *J Affect Disord*, 175:441-445. https://doi.org/10.1016/j.jad.2015.01.054

Liao W, Qiu CJ, Gentili C, et al., 2010. Altered effective connectivity network of the amygdala in social anxiety disorder: a resting-state fMRI study. *PLoS ONE*, 5(12): e15238. https://doi.org/10.1371/journal.pone.0015238

Liu HG, Qin W, Qi HT, et al., 2015. Parcellation of the human orbitofrontal cortex based on gray matter volume covariance. *Hum Brain Mapp*, 36(2):538-548. https://doi.org/10.1002/hbm.22645

Maddock RJ, Garrett AS, Buonocore MH, 2003. Posterior cingulate cortex activation by emotional words: fMRI evidence from a valence decision task. *Hum Brain Mapp*, 18(1):30-41. https://doi.org/10.1002/hbm.10075

Milad MR, Rauch SL, 2007. The role of the orbitofrontal cortex in anxiety disorders. *Ann NY Acad Sci*, 1121(1): 546-561. https://doi.org/10.1196/annals.1401.006

Milad MR, Rauch SL, Pitman RK, et al., 2006. Fear extinction in rats: implications for human brain imaging and anxiety disorders. *Biol Psychol*, 73(1):61-71. https://doi.org/10.1016/j.biopsycho.2006.01.008

Newman MEJ, 2006. Modularity and community structure in networks. *Proc Natl Acad Sci USA*, 103(23):8577-8582. https://doi.org/10.1073/pnas.0601602103

Nooner KB, Colcombe SJ, Tobe RH, et al., 2012. The NKI-Rockland Sample: a model for accelerating the pace of discovery science in psychiatry. *Front Neurosci*, 6:152. https://doi.org/10.3389/fnins.2012.00152

Power JD, Barnes KA, Snyder AZ, et al., 2012. Spurious but systematic correlations in functional connectivity MRI networks arise from subject motion. *Neuroimage*, 59(3): 2142-2154. https://doi.org/10.1016/j.neuroimage.2011.10.018

Qiu CJ, Feng Y, Meng YJ, et al., 2015. Analysis of altered

baseline brain activity in drug-naive adult patients with social anxiety disorder using resting-state functional MRI. *Psychiatry Investig*, 12(3):372-380. https://doi.org/10.4306/pi.2015.12.3.372

Raichle ME, MacLeod AM, Snyder AZ, et al., 2001. A default mode of brain function. *Proc Natl Acad Sci USA*, 98(2): 676-682. https://doi.org/10.1073/pnas.98.2.676

Raymond JG, Steele JD, Seriès P, 2017. Modeling trait anxiety: from computational processes to personality. *Front Psychiatry*, 8:1. https://doi.org/10.3389/fpsyt.2017.00001

Scheinost D, Stoica T, Saksa J, et al., 2013. Orbitofrontal cortex neurofeedback produces lasting changes in contamination anxiety and resting-state connectivity. *Transl Psychiatry*, 3(4):e250. https://doi.org/10.1038/tp.2013.24

Shiba Y, Santangelo AM, Roberts AC, 2016. Beyond the medial regions of prefrontal cortex in the regulation of fear and anxiety. *Front Syst Neurosci*, 10:12. https://doi.org/10.3389/fnsys.2016.00012

Shin LM, Liberzon I, 2010. The neurocircuitry of fear, stress, and anxiety disorders. *Neuropsychopharmacology*, 35(1): 169-191. https://doi.org/10.1038/npp.2009.83

Spampinato MV, Wood JN, de Simone V, et al., 2009. Neural correlates of anxiety in healthy volunteers: a voxel-based morphometry study. *J Neuropsychiatry Clin Neurosci*, 21(2):199-205. https://doi.org/10.1176/jnp.2009.21.2.199

Spielberger CD, Gorsuch RL, Lushene RE, 1983. Manual for the State-Trait Anxiety Inventory. Consulting Psychologists Press, Palo Alto, USA.

Tian X, Wei DT, Du X, et al., 2016. Assessment of trait anxiety and prediction of changes in state anxiety using functional brain imaging: a test–retest study. *NeuroImage*, 133:408-416. https://doi.org/10.1016/j.neuroimage.2016.03.024

Tzourio-Mazoyer N, Landeau B, Papathanassiou D, et al., 2002. Automated anatomical labeling of activations in SPM using a macroscopic anatomical parcellation of the MNI MRI single-subject brain. *Neuroimage*, 15(1):273-289. https://doi.org/10.1006/nimg.2001.0978

Wang S, Xu X, Zhou M, et al., 2017. Hope and the brain: trait hope mediates the protective role of medial orbitofrontal cortex spontaneous activity against anxiety. *Neuroimage*, 157:439-447. https://doi.org/10.1016/j.neuroimage.2017.05.056

Wang ZQ, Xia MR, Dai ZJ, et al., 2015. Differentially disrupted functional connectivity of the subregions of the inferior parietal lobule in Alzheimer's disease. *Brain Struct Funct*, 220(2):745-762. https://doi.org/10.1007/s00429-013-0681-9

Worsley K, 2001. Statistical analysis of activation images. In: Jezzard P, Matthews PM, Smith SM (Eds.), Functional MRI: an Introduction to Methods. Oxford University Press, New York, USA, p.251-270.

Xia MR, Wang ZQ, Dai ZJ, et al., 2014. Differentially disrupted functional connectivity in posteromedial cortical subregions in Alzheimer's disease. *J Alzheimers Dis*, 39(3):527-543. https://doi.org/10.3233/JAD-131583

Yan CG, Zang YF, 2010. DPARSF: a MATLAB toolbox for "pipeline" data analysis of resting-state fMRI. *Front Syst Neurosci*, 4:13. https://doi.org/10.3389/fnsys.2010.00013

Zang YF, He Y, Zhu CZ, et al., 2007. Altered baseline brain activity in children with ADHD revealed by resting-state functional MRI. *Brain Dev*, 29(2):83-91. https://doi.org/10.1016/j.braindev.2006.07.002

Zhang DY, Raichle ME, 2010. Disease and the brain's dark energy. *Nat Rev Neurol*, 6(1):15-28. https://doi.org/10.1038/nrneurol.2009.198

Zhao XH, Wang PJ, Li CB, et al., 2007. Altered default mode network activity in patient with anxiety disorders: an fMRI study. *Eur J Radiol*, 63(3):373-378. https://doi.org/10.1016/j.ejrad.2007.02.006

Zou QH, Zhu CZ, Yang YH, et al., 2008. An improved approach to detection of amplitude of low-frequency fluctuation (ALFF) for resting-state fMRI: fractional ALFF. *J Neurosci Methods*, 172(1):137-141. https://doi.org/10.1016/j.jneumeth.2008.04.012

Zuo XN, di Martino A, Kelly C, et al., 2010. The oscillating brain: complex and reliable. *Neuroimage*, 49(2):1432-1445. https://doi.org/10.1016/j.neuroimage.2009.09.037

## 中文概要

**题　目：成年男性特质型焦虑与内侧眶额的自发活动有关**

**目　的：**研究内侧眶额与焦虑加工的关系。

**创新点：**采用 Louvain 网络模块检测方法对大脑内侧眶额进行自动化功能亚区分割，并发现内侧眶额与健康成年男性特质型焦虑的关系。

**方　法：**采用静息态低频振幅比率（fALFF）、静息态功能连通性（RSFC）和脑区功能亚区自动化分割方法。

**结　论：**成年男性特质型焦虑分数与内侧眶额的 fALFF 指标间存在显著相关性，并与右脑内侧眶额和楔前叶之间的功能连通性有关。因此，可以认为内侧眶额涉及特质型焦虑加工。

**关键词：**特质型焦虑；低频振幅比率；内侧眶额；楔前叶；功能连通性